Theoretical oscillator strengths for spin-allowed electric-dipole transitions in Zn-like ions

Hsin-Chang Chi[1,3] and Hsiang-Shun Chou[2,3]

[1]*Department of Physics, National Dong Hwa University, 1, Sec 2, Da Hsueh Road, Shou-Feng, Hualien, Taiwan 974, Republic of China*

[2]*Institute of Optoelectronic Sciences, National Taiwan Ocean University, Keelung, Taiwan 202, Republic of China*

[3]*National Center for Theoretical Sciences, Taipei, Taiwan 106, Republic of China*

(Received 16 April 2010; published 30 September 2010)

We have performed a relativistic many-body perturbation theory calculation up to second order to study the transition amplitudes, Einstein *A* coefficients, and oscillator strengths for the spin-allowed electric-dipole transitions in the Zn-like ions Zn, Ge^{2+}, As^{3+}, Kr^{6+}, Nb^{11+}, and Mo^{12+}. All possible transitions among the first 13 levels of these ions have been studied. The total transition amplitudes obtained in different gauges are in excellent agreement. The gauge dependences of the first and second order, and the total transition amplitudes are derived. A theoretical justification for the small gauge dependence of the total transition amplitude is given. The present calculations agree well with experiment for all ions except for the neutral Zn atom.

DOI: 10.1103/PhysRevA.82.032518 PACS number(s): 32.70.Cs, 31.15.vj, 31.15.ag

I. INTRODUCTION

The calculation of oscillator strengths for transitions in highly charged ions is one of the most fascinating problems in atomic physics. Both correlation and relativistic effects are important in highly charged ions. Reliable relativistic atomic many-body calculations are required to determine the oscillator strengths in highly charged ions. In this paper, we present a systematic study of oscillator strengths for the spin-allowed electric-dipole (*E*1) transitions in the Zn-like ions. Many calculations have been carried out for oscillator strengths in the Zn-like ions. Among others, several approaches are relativistic random-phase approximation (RRPA) calculations [1,2], first-order theory of oscillator strength (FOTOS) [3], multiconfiguration Hartree-Fock (MCHF) calculations [4–7], relativistic Hartree-Fock (HFR) calculations [8,9], semiempirical model-potential (MP) methods [10], multiconfiguration Dirac-Fock (MCDF) calculations [11–15], configuration interaction (CI) calculations [13,16–20], multiconfiguration relativistic random-phase approximation (MCRRPA) calculations [21–23], relativistic quantum defect orbital (RQDO) calculations [24,25], and empirical prediction methods [26]. Many experiments have been performed to measure the lifetimes of the Zn-like ions [27–35].

We have derived the second-order relativistic many-body perturbation theory (RMBPT) formulas [36] for transition amplitudes in atoms with two valence electrons. The RMBPT provides an *ab initio* and systematic method for treating the correlation effects in atoms. The contribution from higher-order correlation corrections decrease rapidly as nuclear charges increase; therefore, the RMBPT treatment of correlation effects becomes essentially exact for highly charged ions. The second-order RMBPT formulas have been applied to study the spin-allowed *E*1 transitions in the Be-like ions [36–38]. The transition amplitudes obtained in different gauges are in excellent agreement. In addition, the RMBPT transition amplitudes agree well with experiment for all ions except for the neutral Be atom. In this paper, we perform RMBPT calculations up to second order to calculate the transition amplitudes, Einstein *A* coefficients and oscillator strengths for the spin-allowed *E*1 transitions in the Zn-like ions Zn, Ge^{2+}, As^{3+}, Kr^{6+}, Nb^{11+}, and Mo^{12+}. There are 16 spin-allowed *E*1 transitions among the first 13 levels of the Zn-like ions. They are $(4s^2)\ ^1S_0 \rightarrow (4s4p)\ ^1P_1^o$, $(4s4p)\ ^3P_1^o \rightarrow (4p^2)\ ^3P_0$, $(4s4p)\ ^1P_1^o \rightarrow (4p^2)\ ^1S_0$, $(4s4p)\ ^3P_0^o \rightarrow (4p^2)\ ^3P_1$, $(4s4p)\ ^3P_1^o \rightarrow (4p^2)\ ^3P_1$, $(4s4p)\ ^3P_2^o \rightarrow (4p^2)\ ^3P_1$, $(4s4p)\ ^1P_1^o \rightarrow (4p^2)\ ^1D_2$, $(4s4p)\ ^3P_1^o \rightarrow (4p^2)\ ^3P_2$, $(4s4p)\ ^3P_2^o \rightarrow (4p^2)\ ^3P_2$, $(4s4p)\ ^3P_0^o \rightarrow (4s4d)\ ^3D_1$, $(4s4p)\ ^3P_1^o \rightarrow (4s4d)\ ^3D_1$, $(4s4p)\ ^3P_2^o \rightarrow (4s4d)\ ^3D_1$, $(4s4p)\ ^3P_1^o \rightarrow (4s4d)\ ^3D_2$, $(4s4p)\ ^3P_2^o \rightarrow (4s4d)\ ^3D_2$, $(4s4p)\ ^3P_2^o \rightarrow (4s4d)\ ^3D_3$, and $(4s4p)\ ^1P_1^o \rightarrow (4s4d)\ ^1D_2$. In Sec. II, a short description of the second-order RMBPT formulas is presented. Results and discussion are given in Sec. III.

II. SECOND-ORDER RMBPT FORMULAS

The atomic systems satisfy the Schrödinger equation

$$H|\Psi\rangle = E|\Psi\rangle, \tag{2.1}$$

where H is the "no-pair" Hamiltonian given by

$$H = H_0 + V_I. \tag{2.2}$$

In second-quantized form,

$$H_0 = \sum_i \epsilon_i a_i^\dagger a_i \tag{2.3}$$

and

$$V_I = \frac{1}{2}\sum_{ijkl} g_{ijkl} a_i^\dagger a_j^\dagger a_l a_k - \sum_{ij} U_{ij} a_i^\dagger a_j. \tag{2.4}$$

In Eq. (2.3), ϵ_i is the eigenvalue of the one-electron Dirac equation

$$h(\vec{r})u_i(\vec{r}) = \epsilon_i u_i(\vec{r}), \tag{2.5}$$

where the Dirac Hamiltonian $h(\vec{r})$ is given by

$$h(\vec{r}) = c\vec{\alpha}\cdot\vec{p} + \beta c^2 + V_{\rm nuc}(r) + U(r). \tag{2.6}$$

In Eq. (2.4), the sum is over positive-energy states only. Atomic units (a.u.) are employed in this paper. The nuclear Coulomb potential $V_{\rm nuc}(r)$ in general includes the effect of the finite size of the nucleus. The model potential $U(r)$ accounts approximately for the effect of the electron-electron interactions. In the present calculations, we choose $U(r)$ to be

the frozen-core Dirac-Fock potential. In Eq. (2.4), U_{ij} is the one-electron matrix element of $U(r)$,

$$U_{ij} = \int d^3r\, u_i^\dagger(\vec{r}) U(r) u_j(\vec{r}), \tag{2.7}$$

and g_{ijkl} is the Coulomb integral

$$g_{ijkl} = \int d^3r\, d^3r' \frac{1}{|\vec{r} - \vec{r}\,'|} u_i^\dagger(\vec{r}) u_k(\vec{r}) u_j^\dagger(\vec{r}\,') u_l(\vec{r}\,'). \tag{2.8}$$

The Breit interaction is omitted in the present calculations because it is not important for the spin-allowed $E1$ transitions.

We expand the exact wave function $|\Psi\rangle$ and the exact energy E in powers of V_I:

$$E = E^{(0)} + E^{(1)} + \cdots, \tag{2.9}$$

$$|\Psi\rangle = |\Psi^{(0)}\rangle + |\Psi^{(1)}\rangle + \cdots. \tag{2.10}$$

Substitution of Eqs. (2.9) and (2.10) into (2.1) gives

$$(H_0 - E^{(0)})|\Psi^{(0)}\rangle = 0 \tag{2.11}$$

and

$$(H_0 - E^{(0)})|\Psi^{(1)}\rangle = (E^{(1)} - V_I)|\Psi^{(0)}\rangle. \tag{2.12}$$

We now specialize the discussion to atoms with two valence electrons outside a closed core. The zeroth-order wave function describing an atomic state with angular momentum JM may be written as

$$\left|\Psi_{JM}^{(0)}\right\rangle = \sum_{(vw)\in P} C_{vw} \left|\Phi_{vw}^{(0)}\right\rangle, \tag{2.13}$$

where C_{vw} and $|\Phi_{vw}^{(0)}\rangle$ are the configuration weight coefficients and the configuration wave functions, respectively. The configuration weight coefficients are the eigenvectors of the effective Hamiltonian $H_{\rm eff}$ as defined by Eq. (2.17) in [36]. In the present calculations, we are interested in the first-order and the second-order transition amplitudes. It suffices to diagonalize the first-order effective Hamiltonian as given by Eq. (2.24) in [36]. The configurations included in the zeroth-order wave function span the model space P. In the present calculations, we include all possible configurations within the $n = 4$ complex in the model space. Multiconfiguration wave functions are employed to account for the valence-valence correlations within the $n = 4$ valence shell. The remaining valence-valence correlations, the core-valence, and the core-core correlations are treated by perturbation. It is possible in this way to take into account strongly interacting configurations to all orders and treat the weakly interacting ones by means of low-order perturbation.

The transition amplitude is the reduced matrix element of the transition operator

$$T(\omega) = \sum_{ij} \langle i|\, t(\omega)\, |j\rangle\, a_i^\dagger a_j, \tag{2.14}$$

where $t(\omega)$ is the transition operator for one electron and ω is the photon energy. The photon energy can also be expanded in powers of V_I:

$$\omega = \omega^{(0)} + \delta\omega^{(1)} + \cdots, \tag{2.15}$$

where $\omega^{(0)}$ is the zeroth-order photon energy, while $\delta\omega^{(1)}$ is the first-order correction to the photon energy. Consequently, the transition operator can be expanded in powers of V_I:

$$T(\omega) = T^{(0)}(\omega) + T^{(1)}(\omega) + \cdots, \tag{2.16}$$

where

$$T^{(0)}(\omega) = T(\omega^{(0)}) \tag{2.17}$$

and

$$T^{(1)}(\omega) = \delta\omega^{(1)} \frac{dT(\omega^{(0)})}{d\omega}. \tag{2.18}$$

The first-order transition amplitude is given by

$$\langle F||T(\omega)||I\rangle^{(1)} = \left\langle \Psi_F^{(0)}\middle|\middle|T(\omega^{(0)})\middle|\middle|\Psi_I^{(0)}\right\rangle. \tag{2.19}$$

The second-order transition amplitude is

$$\begin{aligned}\langle F||T(\omega)||I\rangle^{(2)} &= \left\langle \Psi_F^{(1)}\middle|\middle|T(\omega^{(0)})\middle|\middle|\Psi_I^{(0)}\right\rangle + \left\langle \Psi_F^{(0)}\middle|\middle|T(\omega^{(0)})\middle|\middle|\Psi_I^{(1)}\right\rangle \\ &\quad + \delta\omega^{(1)} \left\langle \Psi_F^{(0)}\middle|\middle|\frac{dT(\omega^{(0)})}{d\omega}\middle|\middle|\Psi_I^{(0)}\right\rangle,\end{aligned} \tag{2.20}$$

where the third term is the derivative term. The first-order and the second-order transition amplitudes are then expressed in terms of the radial orbital wave functions suitable for numerical evaluations (see Appendix A). The second-order transition amplitude contains four parts: the second-order valence-valence correlation corrections, the second-order RPA corrections, the derivative terms, and the Dirac-Fock terms. The Dirac-Fock terms vanish if we choose the model potential to be the frozen-core Dirac-Fock potential. The absorption oscillator strength is given by

$$f_{FI} = \frac{6c^2}{\omega\,[J_I]} |\langle F||T(\omega)||I\rangle|^2, \tag{2.21}$$

where $[J_I] = 2J_I + 1$. In Eq. (2.21), I and F are the lower and the upper levels, respectively. The Einstein A coefficient for the emission process from F to I is given by

$$A = \frac{2\omega^2}{c^3} \frac{[J_I]}{[J_F]} f_{FI}. \tag{2.22}$$

III. RESULTS AND DISCUSSION

We have calculated the transition amplitudes, Einstein A coefficients and oscillator strengths for all spin-allowed $E1$ transitions among the first 13 levels of the Zn-like ions Zn, Ge^{2+}, As^{3+}, Kr^{6+}, Nb^{11+}, and Mo^{12+}. Contributions to the transition amplitudes of the transitions $(4s4d)\ ^3D_1 \rightarrow (4s4p)\ ^3P_1^o$, $(4s4d)\ ^3D_2 \rightarrow (4s4p)\ ^3P_2^o$, and $(4s4p)\ ^1P_1^o \rightarrow (4s^2)\ ^1S_0$ are given in Table I. The first four rows give the first-order transition amplitudes, the second-order valence-valence corrections, the second-order RPA corrections, and the second-order derivative terms corrections. The last row gives the total transition amplitudes, which are the sums of all rows. The transition amplitudes from the present calculations are accurate to better than 0.1%. In the first-order calculation, we performed a $V^{(N-2)}$ frozen-core Dirac-Fock calculation. Thus the Dirac-Fock terms in the second-order transition amplitude vanish. The derivative terms are seen to contribute substantially to the length results, but have no contributions to the velocity results. The first-order and the total transition amplitudes

TABLE I. Contributions to the transition amplitudes (in a.u.) for the spin-allowed $E1$ transitions in Zn-like ions. Numbers in brackets denote powers of 10. Here T1, Val2, RPA2, and $\delta\omega^{(1)}$ represent the first-order transition amplitudes, the second-order valence-valence corrections, the second-order RPA corrections, and the second-order derivative terms corrections, respectively. L and V indicate the length and the velocity results.

		$(4s4d)\,^3D_1 \rightarrow (4s4p)\,^3P_1^o$		$(4s4d)\,^3D_2 \rightarrow (4s4p)\,^3P_2^o$		$(4s4p)\,^1P_1^o \rightarrow (4s^2)\,^1S_0$	
Ions		L	V	L	V	L	V
Zn	T1	−1.045[−3]	−1.140[−3]	1.040[−3]	1.135[−3]	−1.637[−3]	−2.167[−3]
	Val2	−3.111[−5]	3.331[−4]	3.215[−5]	−3.285[−4]	−2.000[−4]	1.762[−4]
	RPA2	3.365[−5]	1.683[−5]	−3.298[−5]	−1.653[−5]	1.294[−4]	1.055[−4]
	$\delta\omega^{(1)}$	2.599[−4]	0	−2.576[−4]	0	−2.107[−4]	0
	Total	−7.827[−4]	−7.900[−4]	7.812[−4]	7.897[−4]	−1.917[−3]	−1.885[−3]
Ge^{2+}	T1	−1.790[−3]	−1.890[−3]	1.787[−3]	1.888[−3]	2.229[−3]	2.788[−3]
	Val2	−6.500[−5]	1.327[−4]	6.596[−5]	−1.282[−4]	1.127[−4]	−1.040[−4]
	RPA2	8.464[−5]	5.005[−5]	−8.396[−5]	−5.010[−5]	−1.713[−4]	−1.414[−4]
	$\delta\omega^{(1)}$	7.213[−5]	0	−6.886[−5]	0	3.925[−4]	0
	Total	−1.698[−3]	−1.707[−3]	1.700[−3]	1.710[−3]	2.563[−3]	2.543[−3]
As^{3+}	T1	2.050[−3]	2.155[−3]	2.036[−3]	2.143[−3]	−2.451[−3]	−3.010[−3]
	Val2	6.559[−5]	−8.143[−5]	6.601[−5]	−7.692[−5]	−1.152[−4]	6.392[−5]
	RPA2	−1.022[−4]	−6.499[−5]	−1.006[−4]	−6.471[−5]	1.812[−4]	1.498[−4]
	$\delta\omega^{(1)}$	−2.325[−5]	0	−1.870[−5]	0	−4.252[−4]	0
	Total	1.991[−3]	2.008[−3]	1.983[−3]	2.001[−3]	−2.810[−3]	−2.796[−3]
Kr^{6+}	T1	−2.593[−3]	−2.713[−3]	−2.551[−3]	−2.677[−3]	−2.969[−3]	−3.522[−3]
	Val2	−8.881[−5]	2.064[−5]	−8.705[−5]	7.964[−6]	−8.499[−5]	4.628[−5]
	RPA2	1.346[−4]	1.003[−4]	1.310[−4]	9.954[−5]	1.967[−4]	1.653[−4]
	$\delta\omega^{(1)}$	−5.780[−5]	0	−6.621[−5]	0	−4.748[−4]	0
	Total	−2.605[−3]	−2.592[−3]	−2.573[−3]	−2.570[−3]	−3.332[−3]	−3.310[−3]
Nb^{11+}	T1	−3.107[−3]	−3.244[−3]	3.010[−3]	3.166[−3]	3.602[−3]	4.143[−3]
	Val2	−5.855[−5]	−1.330[−5]	5.721[−5]	1.906[−5]	6.952[−5]	−2.811[−6]
	RPA2	1.547[−4]	1.352[−4]	−1.477[−4]	−1.340[−4]	−2.059[−4]	−1.801[−4]
	$\delta\omega^{(1)}$	−1.090[−4]	0	1.293[−4]	0	5.019[−4]	0
	Total	−3.119[−3]	−3.122[−3]	3.049[−3]	3.051[−3]	3.968[−3]	3.960[−3]
Mo^{12+}	T1	−3.181[−3]	−3.319[−3]	3.073[−3]	3.234[−3]	−3.713[−3]	−4.250[−3]
	Val2	−5.669[−5]	−1.884[−5]	5.520[−5]	2.458[−5]	−6.704[−5]	2.546[−6]
	RPA2	1.563[−4]	1.397[−4]	−1.486[−4]	−1.385[−4]	2.068[−4]	1.822[−4]
	$\delta\omega^{(1)}$	−1.133[−4]	0	1.371[−4]	0	−5.027[−4]	0
	Total	−3.195[−3]	−3.198[−3]	3.116[−3]	3.120[−3]	−4.076[−3]	−4.066[−3]

increase with the nuclear charge. However, the percentages of the second-order corrections to the total transition amplitudes decrease with nuclear charges. It is noticed that the RPA corrections always reduce the transition amplitudes. A simple physical interpretation can be given. The second-order RPA correction to the transition amplitude is the product of the zeroth-order photon energy and the matrix element of the electromagnetic dipole potential. The RPA corrections account for the core-shielding (CS) effects in atoms. The external field induces an internal field inside the atom which shields the external field. Therefore, the CS effects lead to an effective potential that weakens the electromagnetic dipole potential and reduces the dipole-moment matrix elements.

Significant differences are observed between the length results and the velocity results of the first−order transition amplitudes. In Appendix B, we study the gauge dependence of the transition amplitude. The gauge dependence $\langle F||\Delta T||I\rangle^{(1)}$ of the first−order transition amplitude is given by Eq. (B8). Note that $\langle F||\Delta T||I\rangle^{(1)}$ is zeroth order in V_I. It follows from Eq. (B8) that the first-order transition amplitude is gauge independent, provided we start from a local potential. The gauge dependence of the first-order transition amplitudes from the present calculations is due to the fact that we start from a *nonlocal* frozen-core Dirac-Fock potential. It can be seen from Table I that the gauge dependence $\langle F||\Delta T||I\rangle^{(1)}$ of the resonance transition $(4s4p)\,^1P_1^o \rightarrow (4s^2)\,^1S_0$ is greater than those of other transitions. This may be due to the very strong interaction between the $(4s^2)$ and $(4p^2)$ configurations. It deserves further investigations to gain deeper insights into the large gauge dependence $\langle F||\Delta T||I\rangle^{(1)}$ of the resonance transition.

Significant differences are also observed between the length results and the velocity results of the second-order transition amplitudes. The gauge dependence $\langle F||\Delta T||I\rangle^{(2)}$ of the second-order transition amplitude is given by Eq. (B13). The first term in Eq. (B13) is zeroth order in V_I, while other terms are first order. In Appendix B, we show that the second-order transition amplitude is gauge independent, provided one starts from a local potential and artificially includes the contributions from the negative-energy states. In summary, the RMBPT calculations are gauge independent order by order

for calculations starting from a local potential and including the contributions from the negative-energy states. The gauge dependence $\langle F||\Delta T||I\rangle^{(2)}$ in the present calculations is a result of the nonlocality of the model potential and the restriction to positive-energy states in the no-pair Hamiltonian. Despite the significant gauge dependences $\langle F||\Delta T||I\rangle^{(1)}$ and $\langle F||\Delta T||I\rangle^{(2)}$, Table I shows that the inclusion of the second-order transition amplitudes brings the length results and the velocity results into excellent agreement. A theoretical justification goes as follows. The gauge dependence $\langle F||\Delta T||I\rangle^{(1)+(2)}$ of the total transition amplitude, which is the sum of $\langle F||\Delta T||I\rangle^{(1)}$ and $\langle F||\Delta T||I\rangle^{(2)}$, is given by Eq. (B14). An inspection of Eqs. (B8) and (B13) shows that the zeroth-order term of $\langle F||\Delta T||I\rangle^{(2)}$ compensates exactly for $\langle F||\Delta T||I\rangle^{(1)}$. Consequently, the gauge dependence $\langle F||\Delta T||I\rangle^{(1)+(2)}$ of the total transition amplitude is first order in V_I. This is the reason why the inclusion of the second-order correction substantially reduces the gauge dependence of the transition amplitude. In Appendix B, we show that the total transition amplitude is gauge independent, provided we start from a local potential and artificially include the contributions from the negative-energy states. The remaining gauge dependence $\langle F||\Delta T||I\rangle^{(1)+(2)}$ in the present calculations is a result of the nonlocality of the model potential and the restriction to positive-energy states in the no-pair Hamiltonian. It is stressed that the gauge dependence $\langle F||\Delta T||I\rangle^{(1)+(2)}$ of the total transition amplitude is only related to the nonlocality of the model potential and the restriction to positive-energy states. It is not related to the correlations beyond second order. Therefore, there is no possibility that the small gauge dependence $\langle F||\Delta T||I\rangle^{(1)+(2)}$ comes from a fortuitous almost cancellation between the contributions from the negative-energy states and those from the correlations beyond second order. The contributions of the negative-energy states to the transition amplitudes of the Zn-like ions deserves further investigations.

The Einstein A coefficients for the resonance transition in the Zn-like ions are presented in Table II. The length results are tabulated. The Einstein A coefficients from the present calculations are accurate to better than 1%. The present

TABLE II. The Einstein A coefficients (10^9 s^{-1})for the resonance transition $(4s4p)\ ^1P_1^o \rightarrow (4s^2)\ ^1S_0$ in the Zn-like ions. The length results are tabulated.

Method	Zn	Ge^{2+}	As^{3+}	Kr^{6+}	Nb^{11+}	Mo^{12+}
Present	0.946	3.31	4.85	10.4	23.6	26.8
RRPA[a]						26.3
FOTOS[b]						29.9
MCHF[c]	0.758	3.27	4.76	10.4		27.3
HFR[d]					25.4	28.9
HFR[e]				12.0		30.0
Semiempirical MP[f]	0.765				23.5	28.5
CI[g]				8.462	17.36	19.36
MCDF[h]	0.7599	3.171	4.636	10.1	22.8	26.0
MCRRPA[i]		3.411	4.943	10.5	23.5	26.7
Empirical prediction[j]		3.30	4.69	9.80	21.9	25.0
Expt.	0.73 ± 0.02[q]	3.4 ± 0.4[k]	4.3 ± 0.6[k]	9.9 ± 1.0[n]	16 ± 1[o]	
	0.71 ± 0.02[r]	2.7 ± 0.1[m]	3.8 ± 0.7[l]		25 ± 3[p]	
	0.69 ± 0.07[s]					
	0.70 ± 0.07[t]					

[a]Reference [1].
[b]Reference [3].
[c]Reference [4].
[d]Reference [8].
[e]Reference [9].
[f]Reference [10].
[g]Reference [18].
[h]Reference [15].
[i]Reference [23].
[j]Reference [26] (semiempirical parametrizations).
[k]Reference [27].
[l]Reference [28].
[m]Reference [29].
[n]Reference [30].
[o]Reference [31] (ANDC analysis).
[p]Reference [31] (simulation analysis).
[q]Reference [32].
[r]Reference [33].
[s]Reference [34].
[t]Reference [35].

results agree well with the MCHF [4], MCDF [15], and MCRRPA [23] calculations for all ions except for the neutral Zn atom. In particular, the present results are in excellent agreement with the MCRRPA calculations for highly charged ions Kr^{6+}, Nb^{11+}, and Mo^{12+}. This is as expected because the MCRRPA calculations include the valence-valence and the RPA corrections as well. The A coefficients from the present calculations are much larger than those from the CI calculations [18], but are much smaller than those from the HFR calculations [8,9]. For Ge^{2+} and As^{3+}, all available calculations agree with the experimental results in [27] within the experimental error bars, but disagree with those in [28,29]. For Kr^{6+}, all calculations except for the HFR [9] and the CI [18] calculations agree well with experiment [30]. For Nb^{11+}, all calculations except for the CI [18] calculations are in close agreement with the experimental result from simulation analysis [31], but disagree with that from the arbitrarily normalized decay curve (ANDC) analysis. The CI calculations disagree with the experimental results from both analyses. A discrepancy is observed between the present calculations and experiment for the A coefficient of the Zn atom. This is due to the omission of the correlations beyond second order in the present calculations. The comparison of the present results with experiment is shown in Fig. 1.

The oscillator strengths for other transitions in the Zn-like ions are presented in Table III. The oscillator strengths from the present calculations are accurate to better than 1%. The present results agree well with the CI calculations [17], and

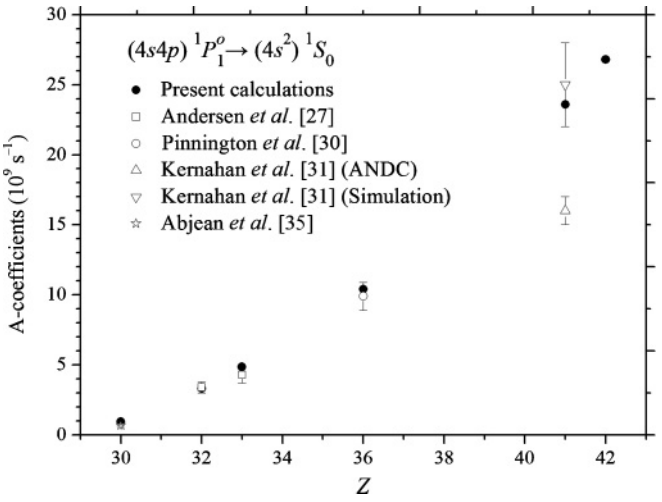

FIG. 1. Plot of the A coefficients from experiment and present calculations for the resonance transition $(4s4p)\ ^1P_1^o \rightarrow (4s^2)\ ^1S_0$ in the Zn-like ions. The data are given in Table II.

are in reasonable agreement with the HFR calculations [8] except for the transition $(4s4p)\ ^3P_0^o \rightarrow (4p4d)\ ^3D_1$ in Nb^{11+} and Mo^{12+}. In addition, the present results are in excellent agreement with the MCHF calculations [5] for the transition $(4s4p)\ ^1P_1^o \rightarrow (4s4d)\ ^1D_2$ in Kr^{6+} and Mo^{12+}. However, significant differences exist between the present results and the MCHF calculations for the transition $(4s4p)\ ^1P_1^o \rightarrow (4p^2)$

TABLE III. The oscillator strengths for the spin-allowed $E1$ transitions in Zn-like ions. The length results are tabulated. Numbers in brackets denote powers of 10. I, the present calculations; II, other theories.

	Ge^{2+}		As^{3+}		Kr^{6+}		Nb^{11+}		Mo^{12+}	
Transitions	I	II	I	II	I	II	I	II	I	II
$(4s4p)\ ^3P_1^o \rightarrow (4p^2)\ ^3P_0$	1.86[−1]		1.86[−1]		1.73[−1]	1.65[−1][e]	1.52[−1]	1.66[−1][c]	1.48[−1]	1.62[−1][c]
$(4s4p)\ ^1P_1^o \rightarrow (4p^2)\ ^1S_0$			2.15[−1]		1.98[−1]	1.81[−1][e]	1.74[−1]	1.90[−1][c]	1.70[−1]	1.81[−1][a]
								2.26[−1][d]		1.85[−1][c]
$(4s4p)\ ^3P_0^o \rightarrow (4p^2)\ ^3P_1$	5.77[−1]		5.77[−1]		5.49[−1]	5.19[−1][e]	5.05[−1]	5.52[−1][c]	4.97[−1]	5.42[−1][c]
$(4s4p)\ ^3P_1^o \rightarrow (4p^2)\ ^3P_1$	1.42[−1]		1.42[−1]		1.34[−1]	1.27[−1][e]	1.20[−1]	1.31[−1][c]	1.18[−1]	1.28[−1][c]
$(4s4p)\ ^3P_2^o \rightarrow (4p^2)\ ^3P_1$	1.37[−1]		1.36[−1]		1.27[−1]	1.22[−1][e]	1.12[−1]	1.24[−1][c]	1.09[−1]	1.20[−1][c]
$(4s4p)\ ^1P_1^o \rightarrow (4p^2)\ ^1D_2$					1.28[−1]	2.40[−1][b]	1.35[−1]	1.68[−1][c]	1.35[−1]	2.15[−1][b]
								5.00[−3][d]		1.66[−1][c]
										3.16[−1][d]
$(4s4p)\ ^3P_1^o \rightarrow (4p^2)\ ^3P_2$	2.41[−1]		2.31[−1]		1.69[−1]		1.14[−1]	1.08[−1][c]	1.08[−1]	1.03[−1][c]
$(4s4p)\ ^3P_2^o \rightarrow (4p^2)\ ^3P_2$	4.18[−1]		4.06[−1]		3.17[−1]		2.50[−1]	2.58[−1][c]	2.44[−1]	2.54[−1][c]
$(4s4p)\ ^3P_0^o \rightarrow (4s4d)\ ^3D_1$	9.36[−1]		9.72[−1]		9.79[−1]		8.53[−1]	9.51[−1][c]	8.31[−1]	9.25[−1][c]
$(4s4p)\ ^3P_1^o \rightarrow (4s4d)\ ^3D_1$	2.37[−1]		2.44[−1]		2.43[−1]		2.07[−1]	2.28[−1][c]	2.01[−1]	2.21[−1][c]
$(4s4p)\ ^3P_2^o \rightarrow (4s4d)\ ^3D_1$	9.74[−3]		9.93[−3]		9.74[−3]		8.22[−3]	8.89[−3][c]	7.96[−3]	8.59[−3][c]
$(4s4p)\ ^3P_1^o \rightarrow (4s4d)\ ^3D_2$	7.02[−1]		7.26[−1]		7.30[−1]		6.30[−1]	6.98[−1][c]	6.13[−1]	6.77[−1][c]
$(4s4p)\ ^3P_2^o \rightarrow (4s4d)\ ^3D_2$	1.45[−1]		1.48[−1]		1.46[−1]		1.24[−1]	1.35[−1][c]	1.21[−1]	1.30[−1][c]
$(4s4p)\ ^3P_2^o \rightarrow (4s4d)\ ^3D_3$	7.95[−1]		8.20[−1]		8.20[−1]		6.95[−1]	7.53[−1][c]	6.74[−1]	7.28[−1][c]
$(4s4p)\ ^1P_1^o \rightarrow (4s4d)\ ^1D_2$					1.60	1.59[b]	1.33	1.41[c]	1.29	1.26[b]
								1.94[d]		1.36[c]
										1.38[d]

[a]Reference [3] (FOTOS).
[b]Reference [5] (MCHF).
[c]Reference [8] (HFR).
[d]Reference [10] (semiempirical MP).
[e]Reference [17] (CI).

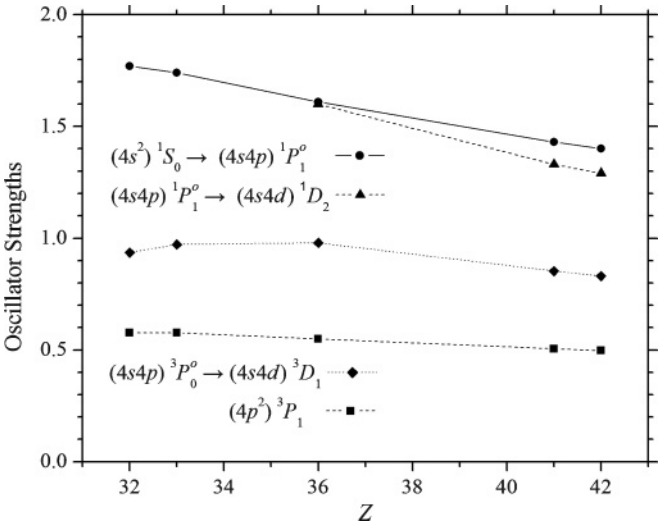

FIG. 2. Plot of the oscillator strengths for the spin-allowed $E1$ transitions $(4s^2)\ ^1S_0 \rightarrow (4s4p)\ ^1P_1^o$, $(4s4p)\ ^1P_1^o \rightarrow (4s4d)\ ^1D_2$, $(4s4p)\ ^3P_0^o \rightarrow (4s4d)\ ^3D_1$, and $(4s4p)\ ^3P_0^o \rightarrow (4p^2)\ ^3P_1$ in the Zn-like ions.

$^1D_2$ in Kr^{6+} and Mo^{12+}. The oscillator strengths as functions of nuclear charges Z are shown in Figs. 2–5. The Z dependences of the oscillator strengths are smooth.

In summary, we perform the RMBPT calculations up to second order to calculate the transition amplitudes, Einstein A coefficients and oscillator strengths for the spin-allowed $E1$ transitions in the Zn-like ions Zn, Ge^{2+}, As^{3+}, Kr^{6+}, Nb^{11+}, and Mo^{12+}. All possible transitions among the first 13 levels of these ions have been studied. The results obtained in different gauges are in excellent agreement. The remaining gauge dependence is due to the nonlocal potential and the exclusion of the negative-energy states. The present calculations agree well with experiment for all ions except for the neutral Zn atom. The accuracy of the present calculations is expected to increase at higher nuclear charges because of the rapid rate of convergence of RMBPT. The discrepancies between experiment and the present calculations are a matter of concern. Further investigations are certainly required to understand fully, and remove, the remaining discrepancies.

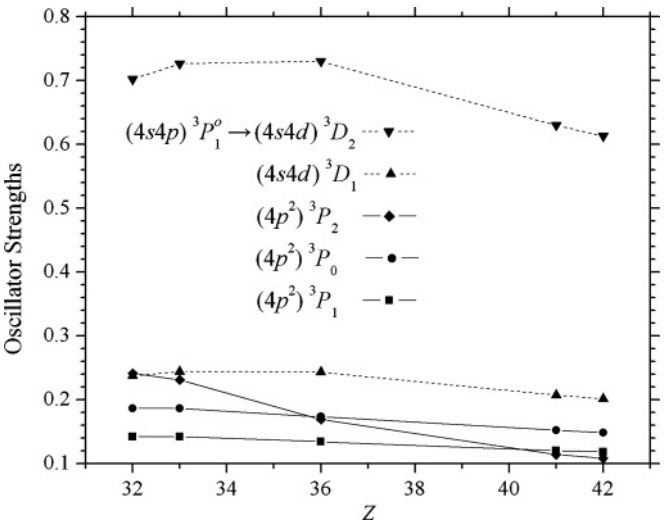

FIG. 3. Plot of the oscillator strengths for the spin-allowed $E1$ transitions $(4s4p)\ ^3P_1^o \rightarrow (4s4d)\ ^3D_2$, $(4s4p)\ ^3P_1^o \rightarrow (4s4d)\ ^3D_1$, $(4s4p)\ ^3P_1^o \rightarrow (4p^2)\ ^3P_2$, $(4s4p)\ ^3P_1^o \rightarrow (4p^2)\ ^3P_0$, and $(4s4p)\ ^3P_1^o \rightarrow (4p^2)\ ^3P_1$ in the Zn-like ions.

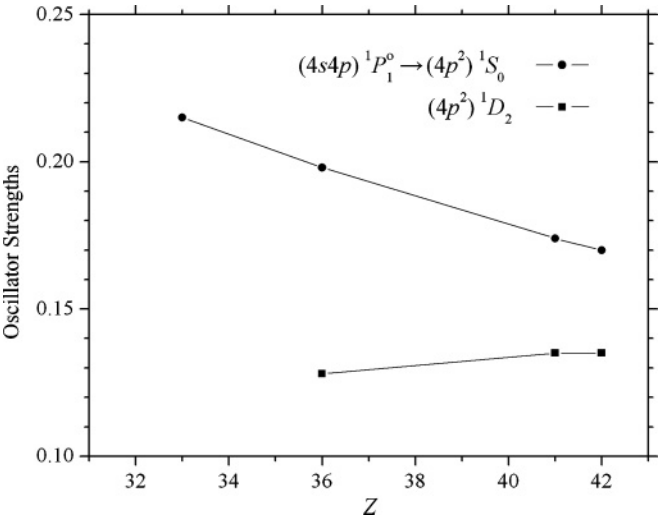

FIG. 4. Plot of the oscillator strengths for the spin-allowed $E1$ transitions $(4s4p)\ ^1P_1^o \rightarrow (4p^2)\ ^1S_0$ and $(4s4p)\ ^1P_1^o \rightarrow (4p^2)\ ^1D_2$ in the Zn-like ions.

APPENDIX A: ANGULAR REDUCTION OF THE RMBPT FORMULAS

The Dirac orbital takes the form

$$u_\alpha(\vec{r}) = \frac{1}{r}\begin{pmatrix} i g_{n_\alpha \kappa_\alpha} \Omega_{\kappa_\alpha m_\alpha} \\ f_{n_\alpha \kappa_\alpha} \Omega_{-\kappa_\alpha m_\alpha} \end{pmatrix}. \tag{A1}$$

We introduce the two-component radial function

$$u_\alpha \equiv u_\alpha(r) \equiv \begin{pmatrix} g_{n_\alpha \kappa_\alpha} \\ f_{n_\alpha \kappa_\alpha} \end{pmatrix}. \tag{A2}$$

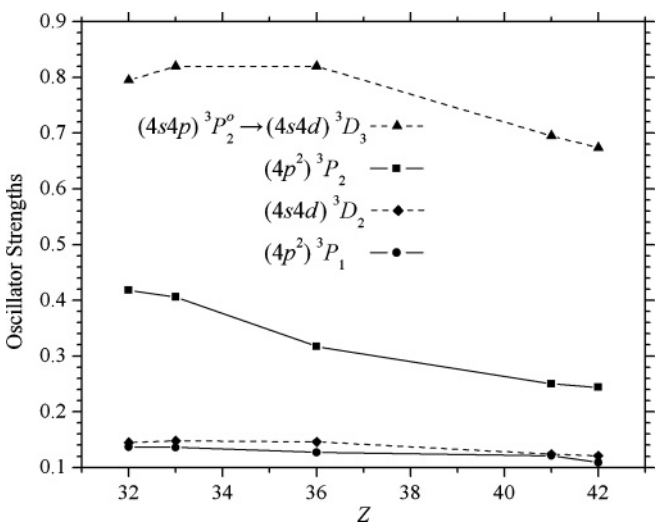

FIG. 5. Plot of the oscillator strengths for the spin-allowed $E1$ transitions $(4s4p)\ ^3P_2^o \rightarrow (4s4d)\ ^3D_3$, $(4s4p)\ ^3P_2^o \rightarrow (4p^2)\ ^3P_2$, $(4s4p)\ ^3P_2^o \rightarrow (4s4d)\ ^3D_2$, and $(4s4p)\ ^3P_2^o \rightarrow (4p^2)\ ^3P_1$ in the Zn-like ions.

The first-order transition amplitude is given by

$$\begin{aligned}\langle F||T(\omega)||I\rangle^{(1)} &= -[J_I]^{1/2}[J_F]^{1/2}\sum_{\substack{(vw)\in P_I\\(v'w')\in P_F}}\eta_{v'w'}\eta_{vw}C_{v'w'}C_{vw}\\ &\times\left((-1)^{J_F+j_v+j_w}\begin{Bmatrix}J_F & J_I & 1\\ j_w & j_{w'} & j_v\end{Bmatrix}\langle w'||t||w\rangle\delta_{vv'}\right.\\ &+(-1)^{J_I+J_F+1}\begin{Bmatrix}J_F & J_I & 1\\ j_v & j_{w'} & j_w\end{Bmatrix}\langle w'||t||v\rangle\delta_{wv'}\\ &+(-1)^{j_{v'}+j_w}\begin{Bmatrix}J_F & J_I & 1\\ j_w & j_{v'} & j_v\end{Bmatrix}\langle v'||t||w\rangle\delta_{vw'}\\ &\left.+\ (-1)^{J_I+j_{v'}+j_{w'}}\begin{Bmatrix}J_F & J_I & 1\\ j_v & j_{v'} & j_w\end{Bmatrix}\langle v'||t||v\rangle\delta_{ww'}\right),\end{aligned}\tag{A3}$$

where

$$\eta_{vw}=\begin{cases}1 & \text{for}\quad v\neq w,\\ 1/\sqrt{2} & \text{for}\quad v=w.\end{cases}\tag{A4}$$

The second-order transition amplitude is given by

$$\begin{aligned}\langle F||T(\omega)||I\rangle^{(2)} &= [J_I]^{1/2}[J_F]^{1/2}\sum_{\substack{(vw)\in P_I\\(v'w')\in P_F}}\eta_{v'w'}\eta_{vw}C_{v'w'}C_{vw}\left[(-1)^{J_I+J_F+1}\sum_{(iv')\notin P_I}\begin{Bmatrix}J_F & J_I & 1\\ j_i & j_{w'} & j_{v'}\end{Bmatrix}\frac{\langle w'||t||i\rangle}{\epsilon_{iv'}-\epsilon_{vw}}Y_{J_I}(i\,v'vw)\right.\\ &+(-1)^{J_I+J_F+1}\sum_{(iw)\notin P_F}\begin{Bmatrix}J_F & J_I & 1\\ j_v & j_i & j_w\end{Bmatrix}\frac{\langle i||t||v\rangle}{\epsilon_{iw}-\epsilon_{v'w'}}Y_{J_F}(v'w'wi)\\ &+\delta_{vv'}(-1)^{j_{v'}+j_{w'}+J_F}\frac{1}{3}\begin{Bmatrix}J_F & J_I & 1\\ j_w & j_{w'} & j_v\end{Bmatrix}\times\left(\sum_{mb}\frac{\langle m||t||b\rangle Z_1(wmw'b)}{\epsilon_{bw'}-\epsilon_{mw}}+\sum_{mb}\frac{Z_1(wbw'm)\langle b||t||m\rangle}{\epsilon_{bw}-\epsilon_{mw'}}\right)\\ &+\delta_{wv'}(-1)^{j_v+j_{w'}+J_I+J_F}\frac{1}{3}\begin{Bmatrix}J_F & J_I & 1\\ j_v & j_{w'} & j_w\end{Bmatrix}\left(\sum_{mb}\frac{\langle m||t||b\rangle Z_1(vmw'b)}{\epsilon_{bw'}-\epsilon_{mv}}+\sum_{mb}\frac{Z_1(vbw'm)\langle b||t||m\rangle}{\epsilon_{bv}-\epsilon_{mw'}}\right)\\ &+\delta_{vv'}(-1)^{j_v+j_w+J_F+1}\begin{Bmatrix}J_F & J_I & 1\\ j_w & j_{w'} & j_v\end{Bmatrix}\left(\sum_{i\neq w'}\delta_{\kappa_i\kappa_{w'}}\frac{\Delta_{w'i}\langle i||t||w\rangle}{\epsilon_{w'}-\epsilon_i}+\sum_{i\neq w}\delta_{\kappa_i\kappa_w}\frac{\langle w'||t||i\rangle\Delta_{iw}}{\epsilon_w-\epsilon_i}\right)\\ &+\delta_{wv'}(-1)^{J_I+J_F+2}\begin{Bmatrix}J_F & J_I & 1\\ j_v & j_{w'} & j_w\end{Bmatrix}\left(\sum_{i\neq w'}\delta_{\kappa_i\kappa_{w'}}\frac{\Delta_{w'i}\langle i||t||v\rangle}{\epsilon_{w'}-\epsilon_i}+\sum_{i\neq v}\delta_{\kappa_i\kappa_v}\frac{\langle w'||t||i\rangle\Delta_{iv}}{\epsilon_v-\epsilon_i}\right)\\ &+\delta\omega^{(1)}\left(\delta_{vv'}(-1)^{j_v+j_w+J_F+1}\begin{Bmatrix}J_F & J_I & 1\\ j_w & j_{w'} & j_v\end{Bmatrix}\langle w'||\frac{dt}{d\omega}||w\rangle+\delta_{wv'}(-1)^{J_I+J_F+2}\begin{Bmatrix}J_F & J_I & 1\\ j_v & j_{w'} & j_w\end{Bmatrix}\langle w'||\frac{dt}{d\omega}||v\rangle\right)\\ &\left.+(-1)^{j_v+j_w+j_{v'}+j_{w'}+J_I+J_F}(1\leftrightarrow 2)\right],\end{aligned}\tag{A5}$$

where $\epsilon_{vw}=\epsilon_v+\epsilon_w$. Here

$$Y_J(abcd)=\sum_k(-1)^{j_b+j_c+k+J}\begin{Bmatrix}j_a & j_b & J\\ j_d & j_c & k\end{Bmatrix}X_k(abcd)\tag{A6}$$

$$+\sum_k(-1)^{j_b+j_c+k}\begin{Bmatrix}j_a & j_b & J\\ j_c & j_d & k\end{Bmatrix}X_k(abdc)\tag{A7}$$

and

$$Z_k(abcd)=X_k(abcd)+\sum_{k'}[k]\begin{Bmatrix}j_a & j_c & k\\ j_b & j_d & k'\end{Bmatrix}X_{k'}(abdc)\tag{A8}$$

with

$$X_k(abcd)=(-1)^k\langle a||C_k||c\rangle\langle b||C_k||d\rangle R_k(abcd).\tag{A9}$$

The quantities C_k are normalized spherical harmonics and $R_k(abcd)$ are Slater integrals. In Eq. (A5), the notation $(1\leftrightarrow 2)$ denotes all preceding terms inside the same brackets with the subscripts 1 and 2 interchanged. It is understood that the indices v and v' in the δ function should be interchanged with w and w', respectively. The first two terms in Eq. (A5) lead to the second-order valence-valence correlation corrections, while the next four terms represent the second-order RPA corrections. The use of frozen-core Dirac-Fock potential leads to a major simplification for Eq. (A5). The Δ_{ij} terms vanish for the forzen-core Dirac-Fock case.

APPENDIX B: GAUGE TRANSFORMATION AND TRANSITION AMPLITUDE

It is convenient to introduce an operator representing the difference between the transition operators in the length and

the velocity gauges,

$$\Delta T = T_l - T_v. \tag{B1}$$

The operator ΔT can be written as

$$\Delta T = \frac{i}{ec}\sqrt{\frac{2\pi}{3}}\Delta H, \tag{B2}$$

where

$$\Delta H = \sum_{ij} \langle i|\, \Delta h_I \,|j\rangle\, a_i^\dagger a_j. \tag{B3}$$

In Eq. (B3), h_I is the interaction Hamiltonian for one electron, and Δh_I is the change of h_I under the gauge transformation. It is straightforward to show that

$$\Delta h_I = -\frac{ie}{\hbar}([h,\chi] - [U_{\rm exc},\chi] - \hbar\omega\chi), \tag{B4}$$

where χ is the gauge function and $U_{\rm exc}$ is the exchange (*nonlocal*) part of the model potential. With the aid of Eq. (B4), Eq. (B3) can be expressed as

$$\Delta H = -\frac{ie}{\hbar}([H_0,X] - \hbar\omega X - [\mathcal{U}_{\rm exc},X]), \tag{B5}$$

where

$$X = \sum_{ij} \langle i|\, \chi \,|j\rangle\, a_i^\dagger a_j \tag{B6}$$

and

$$\mathcal{U}_{\rm exc} = \sum_{ij} \langle i|\, U_{\rm exc} \,|j\rangle\, a_i^\dagger a_j. \tag{B7}$$

The gauge dependence, i.e., the change of the first-order transition amplitude under the gauge transformation, is given by

$$\begin{aligned}
\langle F||\Delta T||I\rangle^{(1)} &= \langle \Psi_F^{(0)}||\Delta T(\omega^{(0)})||\Psi_I^{(0)}\rangle \\
&= \frac{i}{ec}\sqrt{\frac{2\pi}{3}}\langle \Psi_F^{(0)}||\Delta H(\omega^{(0)})||\Psi_I^{(0)}\rangle \\
&= \frac{1}{\hbar c}\sqrt{\frac{2\pi}{3}}\langle \Psi_F^{(0)}||[H_0,X] - \hbar\omega^{(0)}X \\
&\quad - [\mathcal{U}_{\rm exc},X]||\Psi_I^{(0)}\rangle \\
&= \frac{1}{\hbar c}\sqrt{\frac{2\pi}{3}}\langle \Psi_F^{(0)}||\big(E_F^{(0)} - E_I^{(0)} - \hbar\omega^{(0)}\big)X \\
&\quad - [\mathcal{U}_{\rm exc},X]||\Psi_I^{(0)}\rangle \\
&= -\frac{1}{\hbar c}\sqrt{\frac{2\pi}{3}}\langle \Psi_F^{(0)}||[\mathcal{U}_{\rm exc},X]||\Psi_I^{(0)}\rangle.
\end{aligned} \tag{B8}$$

Note that $\langle F||\Delta T||I\rangle^{(1)}$ is zeroth order in V_I. It follows from Eq. (B8) that the first-order transition amplitude is gauge independent, provided we start from a local potential.

The gauge dependence of the second-order transition amplitude is given by

$$\begin{aligned}
&\langle F||\Delta T||I\rangle^{(2)} \\
&\quad = \langle \Psi_F^{(0)}||\Delta T(\omega^{(0)})||\Psi_I^{(1)}\rangle + \langle \Psi_F^{(1)}||\Delta T(\omega^{(0)})||\Psi_I^{(0)}\rangle \\
&\qquad + \delta\omega^{(1)}\langle \Psi_F^{(0)}||\frac{d\Delta T(\omega^{(0)})}{d\omega}||\Psi_I^{(0)}\rangle.
\end{aligned} \tag{B9}$$

With the aid of Eqs. (2.12), (B2), and (B5), the first term in (B9) can be rewritten as

$$\begin{aligned}
&\langle \Psi_F^{(0)}||\Delta T(\omega^{(0)})||\Psi_I^{(1)}\rangle \\
&\quad = \frac{1}{\hbar c}\sqrt{\frac{2\pi}{3}}\langle \Psi_F^{(0)}||[H_0,X] - \hbar\omega^{(0)}X - [\mathcal{U}_{\rm exc},X]||\Psi_I^{(1)}\rangle \\
&\quad = \frac{1}{\hbar c}\sqrt{\frac{2\pi}{3}}\big\{\big(E_F^{(0)} - E_I^{(0)} - \hbar\omega^{(0)}\big)\langle \Psi_F^{(0)}||X||\Psi_I^{(1)}\rangle \\
&\qquad - \langle \Psi_F^{(0)}||X\big(E_I^{(1)} - V_I\big)||\Psi_I^{(0)}\rangle - \langle \Psi_F^{(0)}||[\mathcal{U}_{\rm exc},X]||\Psi_I^{(1)}\rangle\big\} \\
&\quad = -\frac{1}{\hbar c}\sqrt{\frac{2\pi}{3}}\big\{\langle \Psi_F^{(0)}||X\big(E_I^{(1)} - V_I\big)||\Psi_I^{(0)}\rangle \\
&\qquad + \langle \Psi_F^{(0)}||[\mathcal{U}_{\rm exc},X]||\Psi_I^{(1)}\rangle\big\}.
\end{aligned} \tag{B10}$$

The second term in Eq. (B9) can be expressed as

$$\begin{aligned}
&\langle \Psi_F^{(1)}||\Delta T(\omega^{(0)})||\Psi_I^{(0)}\rangle \\
&\quad = \frac{1}{\hbar c}\sqrt{\frac{2\pi}{3}}\langle \Psi_F^{(1)}||[H_0,X] - \hbar\omega^{(0)}X - [\mathcal{U}_{exc},X]||\Psi_I^{(0)}\rangle \\
&\quad = \frac{1}{\hbar c}\sqrt{\frac{2\pi}{3}}\big\{\big(E_F^{(0)} - E_I^{(0)} - \hbar\omega^{(0)}\big)\langle \Psi_F^{(1)}||X||\Psi_I^{(0)}\rangle \\
&\qquad + \langle \Psi_F^{(0)}||\big(E_F^{(1)} - V_I\big)X||\Psi_I^{(0)}\rangle - \langle \Psi_F^{(1)}||[\mathcal{U}_{\rm exc},X]||\Psi_I^{(0)}\rangle\big\} \\
&\quad = \frac{1}{\hbar c}\sqrt{\frac{2\pi}{3}}\big\{\langle \Psi_F^{(0)}||\big(E_F^{(1)} - V_I\big)X||\Psi_I^{(0)}\rangle \\
&\qquad - \langle \Psi_F^{(1)}||[\mathcal{U}_{\rm exc},X]||\Psi_I^{(0)}\rangle\big\}.
\end{aligned} \tag{B11}$$

The third term in Eq. (B9) can be expressed as

$$\begin{aligned}
&\delta\omega^{(1)}\langle \Psi_F^{(0)}||\frac{d\Delta T(\omega^{(0)})}{d\omega}||\Psi_I^{(0)}\rangle \\
&\quad = \frac{1}{\hbar c}\sqrt{\frac{2\pi}{3}}\delta\omega^{(1)}\langle \Psi_F^{(0)}||\left[H_0,\frac{dX}{d\omega}\right] - \hbar\omega^{(0)}\frac{dX}{d\omega} \\
&\qquad - \hbar X - \left[\mathcal{U}_{\rm exc},\frac{dX}{d\omega}\right]||\Psi_I^{(0)}\rangle \\
&\quad = \frac{1}{\hbar c}\sqrt{\frac{2\pi}{3}}\delta\omega^{(1)}\left\{\big(E_F^{(0)} - E_I^{(0)} - \hbar\omega^{(0)}\big)\langle \Psi_F^{(0)}||\frac{dX}{d\omega}||\Psi_I^{(0)}\rangle\right. \\
&\qquad \left. - \hbar\langle \Psi_F^{(0)}||X||\Psi_I^{(0)}\rangle - \langle \Psi_F^{(0)}||\left[\mathcal{U}_{\rm exc},\frac{dX}{d\omega}\right]||\Psi_I^{(0)}\rangle\right\} \\
&\quad = -\frac{1}{\hbar c}\sqrt{\frac{2\pi}{3}}\delta\omega^{(1)}\left\{\hbar\langle \Psi_F^{(0)}||X||\Psi_I^{(0)}\rangle\right. \\
&\qquad \left. + \langle \Psi_F^{(0)}||\left[\mathcal{U}_{\rm exc},\frac{dX}{d\omega}\right]||\Psi_I^{(0)}\rangle\right\}.
\end{aligned} \tag{B12}$$

The sum of Eqs. (B10), (B11), and (B12) is

$$\begin{aligned}
&\langle F||\Delta T||I\rangle^{(2)} \\
&\quad = \frac{1}{\hbar c}\sqrt{\frac{2\pi}{3}}\left\{\big(E_F^{(1)} - E_I^{(1)} - \hbar\delta\omega^{(1)}\big)\langle \Psi_F^{(0)}||X||\Psi_I^{(0)}\rangle\right. \\
&\qquad + \langle \Psi_F^{(0)}||[X,V_I]||\Psi_I^{(0)}\rangle - \langle \Psi_F^{(0)}||[\mathcal{U}_{\rm exc},X]||\Psi_I^{(1)}\rangle \\
&\qquad - \langle \Psi_F^{(1)}||[\mathcal{U}_{\rm exc},X]||\Psi_I^{(0)}\rangle - \delta\omega^{(1)}\langle \Psi_F^{(0)}|| \\
&\qquad \left. \times \left[\mathcal{U}_{\rm exc},\frac{dX}{d\omega}\right]||\Psi_I^{(0)}\rangle\right\}
\end{aligned}$$

$$= \frac{1}{\hbar c}\sqrt{\frac{2\pi}{3}}\Big\{-\langle\Psi_F^{(0)}||[X,\mathcal{U}_{\rm exc}]||\Psi_I^{(0)}\rangle + \langle\Psi_F^{(0)}||[X,V_I+\mathcal{U}_{\rm exc}]||\Psi_I^{(0)}\rangle - \langle\Psi_F^{(0)}||[\mathcal{U}_{\rm exc},X]||\Psi_I^{(1)}\rangle - \langle\Psi_F^{(1)}||[\mathcal{U}_{\rm exc},X]||\Psi_I^{(0)}\rangle - \delta\omega^{(1)}\langle\Psi_F^{(0)}|| \times\left[\mathcal{U}_{\rm exc},\frac{dX}{d\omega}\right]||\Psi_I^{(0)}\rangle\Big\}. \quad \text{(B13)}$$

In Eq. (B13), the first term is zeroth order in V_I, while other terms are first order. It has been shown [39] that the commutator $[X,V_I+\mathcal{U}_{\rm exc}]$ vanishes, provided one *artificially* includes the contributions from the negative-energy states. Therefore, the second-order transition amplitude is gauge independent, provided one starts from a local potential and artificially includes the contributions from the negative-energy states. In summary, the RMBPT calculations are gauge independent order by order for calculations starting from a local potential and including the contributions from the negative-energy states.

The gauge dependence of the total transition amplitude is given by the sum of Eqs. (B8) and (B13):

$$\langle F||\Delta T||I\rangle^{(1)+(2)} = \frac{1}{\hbar c}\sqrt{\frac{2\pi}{3}}\Big\{\langle\Psi_F^{(0)}||[X,V_I+\mathcal{U}_{\rm exc}]||\Psi_I^{(0)}\rangle - \langle\Psi_F^{(0)}||[\mathcal{U}_{\rm exc},X]||\Psi_I^{(1)}\rangle - \langle\Psi_F^{(1)}||[\mathcal{U}_{exc},X]||\Psi_I^{(0)}\rangle - \delta\omega^{(1)}\langle\Psi_F^{(0)}||\left[\mathcal{U}_{\rm exc},\frac{dX}{d\omega}\right]||\Psi_I^{(0)}\rangle\Big\}. \quad \text{(B14)}$$

In arriving at Eq. (B14), the first term in Eq. (B13) compensates exactly for the gauge dependence $\langle F||\Delta T||I\rangle^{(1)}$ in Eq. (B8). Consequently, the gauge dependence $\langle F||\Delta T||I\rangle^{(1)+(2)}$ of the total transition amplitude is first order in V_I. As a result, the inclusion of the second-order correction substantially reduces the gauge dependence of the transition amplitude.

[1] P. Shore and A. Dalgarno, Phys. Rev. A **16**, 1502 (1977).
[2] P. Shore, Phys. Rev. A **18**, 1060 (1978).
[3] D. R. Beck and C. A. Nicolaides, Phys. Lett. A **65**, 293 (1978).
[4] C. Froese Fischer and J. E. Hansen, Phys. Rev. A **17**, 1956 (1978).
[5] C. Froese Fischer and J. E. Hansen, Phys. Rev. A **19**, 1819 (1979).
[6] T. Brage and C. Froese Fischer, Phys. Scr. **45**, 43 (1992).
[7] E. Biémont and M. Godefroid, Phys. Scr. **22**, 231 (1980).
[8] E. Biémont, P. Quinet, and B. C. Fawcett, Phys. Scr. **39**, 562 (1989).
[9] R. D. Cowan, Los Alamos Scientific Lab Report No. LA-6679-MS, 1977 (unpublished).
[10] G. A. Victor and W. R. Taylor, At. Data Nucl. Data Tables **28**, 107 (1983).
[11] J. Bruneau, J. Phys. B **17**, 3009 (1984).
[12] E. Biémont, At. Data Nucl. Data Tables **43**, 163 (1989).
[13] J. Migdalek and M. Stanek, Phys. Rev. A **41**, 2869 (1990).
[14] J. Migdalek and M. Stanek, J. Quant. Spectrosc. Radiat. Transfer **42**, 585 (1989).
[15] Y. Liu, R. Hutton, Y. Zou, M. Anderson, and T. Brage, J. Phys. B **39**, 3147 (2006).
[16] S. S. Tayal, Phys. Scr. **43**, 270 (1991).
[17] A. Hibbert and A. C. Bailie, Phys. Scr. **45**, 565 (1992).
[18] J. Fleming and A. Hibbert, Phys. Scr. **51**, 339 (1995).
[19] T. McElory and A. Hibbert, Phys. Scr. **71**, 479 (2005).
[20] L. Glowacki and J. Migdalek, J. Phys. B **39**, 1721 (2006).
[21] K. N. Huang and W. R. Johnson, Nucl. Instrum. Methods Phys. Res. B **9**, 502 (1985).
[22] T. C. Cheng and K. N. Huang, Phys. Rev. A **45**, 4367 (1992).
[23] H. S. Chou, H. C. Chi, and K. N. Huang, Phys. Rev. A **49**, 2394 (1994).
[24] C. Lavín, P. Martin, and I. Martin, Int. J. Quantum Chem., Symp. **48**, 385 (1993).
[25] E. Charro, I. Marin, and C. Lavín, Astron. Astrophys. Suppl. Ser. **124**, 397 (1997).
[26] L. J. Curtis, J. Opt. Soc. Am. B **9**, 5 (1992).
[27] T. Andersen, P. Eriksen, O. Poulsen, and P. S. Ramanujam, Phys. Rev. A **20**, 2621 (1979).
[28] E. H. Pinnington, J. L. Bahr, J. A. Kernahan, and D. J. G. Irwin, J. Phys. B **14**, 1291 (1981).
[29] E. H. Pinnington, J. L. Bahr, D. J. G. Irwin, and J. A. Kernahan, Nucl. Instrum. Methods **202**, 67 (1982).
[30] E. H. Pinnington, W. Ansbacher, and J. A. Kernahan, J. Opt. Soc. Am. B **1**, 30 (1984).
[31] J. A. Kernahan, E. H. Pinnington, E. J. Doerfert, E. Träbert, J. Granzow, A. Wolf, K. Kenntner, D. Habs, M. Grieser, T. Schubler, U. Schramm, and P. Forck, Nucl. Instrum. Methods Phys. Res. B **98**, 57 (1995).
[32] A. Landman and R. Novick, Phys. Rev. **134**, A56 (1964).
[33] A. Lurio, R. L. deZafra, and R. J. Goshen, Phys. Rev. **134**, A1198 (1964).
[34] T. Andersen and G. Sc6rensen, J. Quant. Spectrosc. Radiat. Transfer **13**, 369 (1973).
[35] R. Abjean and A. Johannin-Gilles, J. Quant. Spectrosc. Radiat. Transfer **15**, 25 (1975).
[36] H. S. Chou, Phys. Rev. A **62**, 042507 (2000).
[37] H. S. Chou, Phys. Scr. **64**, 140 (2001).
[38] P. Bogdanovich and H. S. Chou, Lithuanian J. Phys. **47**, 387 (2007).
[39] W. R. Johnson, D. R. Plante, and J. Sapirstein, Adv. At. Mol. Opt. Phys. **35**, 255 (1995).